CrossMark

ORIGINAL PAPER

Facile electrochemical growth of nanostructured copper phthalocyanine thin film via simultaneous anodic oxidation of copper and dilithium phthalocyanine for photoelectrochemical hydrogen evolution

R. S. Vishwanath[1] · Sakthivel Kandaiah[1]

Abstract We present a novel electrochemical approach to grow copper phthalocyanine (CuPc) thin-film photoelectrodes through anodic oxidation of copper and dilithium phthalocyanine (Li$_2$Pc). This circumvents the challenges associated with the electrochemical processing of unsubstituted CuPc from solution. The potentiostatic co-electrooxidation reaction at the heterogeneous interface favors the growth of CuPc thin film. The surface morphology of thin film exhibits nanorod-like features. UV-Vis, grazing angle Fourier transform infrared (FTIR), and grazing angle X-ray diffraction patterns reveal that the nanocrystalline phase corresponds only to α-CuPc and no admixture of other polymorphs. Photocurrent measurement shows a stable photoresponse in neutral medium. The photoelectrochemical hydrogen evolution on p-type CuPc coated copper photocathode shows an enhanced activity over bare copper and indium tin oxide (ITO) electrodeposited with CuPc and monolithium phthalocyanine radical (LiPc) thin films.

Keywords Photoelectrochemical hydrogen evolution ·
Electrodeposition · Photocathodes · Copper phthalocyanine ·
Dilithium phthalocyanine

Introduction

Solar energy conversion to solar fuels through photoelectrochemical process needs photoactive semiconductors fabricated as thin-film photoelectrodes [1–4]. Nanoarchitectures

✉ Sakthivel Kandaiah
  sakthivel@reva.edu.in

[1] School of Chemical Sciences, REVA University,
    Bangalore, Karnataka 560064, India

of photoelectrodes play a significant role on semiconductor/ electrolyte interface, efficient trapping of the visible part of the solar spectrum, and separation of photogenerated excitons. The long-term stability of the photoactive materials in a three-phase interface for hydrogen evolution is another vital requirement in photoelectrochemical cells [4, 5]. Recently, p-type photoactive polymeric organic semiconductors and molecular photocatalysts as heterojunction with inorganic photoelectrodes were in focus to retard the recombination effects and to enhance the effective separation of photogenerated charge carriers [6–8]. The symmetrical phthalocyanine ligand is an important model for biologically essential species such as chlorophyll, hemoglobin, and porphyrin [9, 10]. The remarkable physio-chemical stability, crystal structure features, and semiconducting behavior of phthalocyanines have extended their application in many vital areas [9, 10]. CuPc is one of the important p-type semiconducting metallo-phthalocyanine (MPc) in the view of its physio-chemical stability, band gap (1.8 eV), and a bright cyan color. This is useful in solar cells, thin-film transistors, light-emitting diodes, and bio-sensing [11–14]. The photoelectrochemistry of many metal phthalocyanines show a good visible light absorption and photoconductivity [15]. It is observed that the photocurrent response of the thin films depends on the molecular ordering, thickness, and the redox characteristics of metal phthalocyanines [16, 17]. Mostly, these thin films were fabricated by physical methods and the photocurrent responses were studied in a dry cell setup [16, 17].

Electrochemical growth of unsubstituted MPcs as thin films from the solution remains seldom explored due to their solubility limitations [9, 10]. Hence, the thin films of CuPc were usually fabricated by high-temperature techniques, ultrahigh vacuum-organic molecular beam deposition, spray coating, spin coating, and precipitation techniques. But, these techniques require the strict control on the thin-film

fabrication parameters which affect the phase formation, surface morphology, and other properties [18]. Generally, phthalocyanine rings were functionalized to improve their solubility [19, 20]. This significantly alters the structural, optical, and electrical properties in thin films.

Thin-film growth by direct electrochemical synthesis on the electrodes is a soft technique. Electrocrystallization method could yield very crystalline solids and highly pure phase of some materials which are difficult to obtain by other synthetic routes [21–23]. Tunable parameters like potential, current density, and electrolytic bath composition have control on surface nanostructure and composition [22, 24, 25]. Among the metal ion containing unsubstituted phthalocyanines, Li_2Pc shows the highest solubility [9, 10, 26]. Two lithium ions in Li_2Pc can be easily replaced by divalent metal ions in solution to form insoluble MPcs. Electrooxidation of Li_2Pc in acetonitrile or acetone produces needle-like LiPc crystals or thin-film on different electrode surfaces [26–28]. LiPc is the first monovalent phthalocyanine radical compound which is a p-type semiconductor and paramagnetic in nature [26]. Electrodeposition of unsubstituted FePc was done with the modification of electrolytic conditions by using ionic liquids [29]. A cathodic electrophoretic deposition of aggregated CuPc film on indium tin oxide (ITO) substrate was done from the protonated-oxidized CuPc in trifluoroacetic acid containing dicholoromethane [30]. Electrodeposition of ring substituted Cu(II), Fe(III), and Al(III) tetrasulphonated phthalocyanine tetrasodium compounds on the gold electrode in alkaline media was reported [18]. Recently, electropolymerization of water-soluble copper (II) phthalocyanine bearing tetrakis(1, 1-(dicarbpentoxy)-2-(4-biphenyl)-ethyl)-tetrachloro substituents, which was denoted by authors as CuPc, was investigated for hydrogen evolution reaction (HER) [20].

Here we describe a new electrochemical methodology for direct preparation of nanostructured, ring unsubstituted CuPc thin film on the copper substrate via simultaneous anodic oxidation of copper and Li_2Pc. In this approach, we make use of the onset electrooxidation potentials of Li_2Pc and copper to prepare CuPc thin films in the organic medium. The photocurrent measurements and photoelectrochemical hydrogen evolution performance of these photocathodes were investigated in neutral and in acidic conditions.

Experimental

Dilithium phthalocyanine (Li_2Pc; Aldrich), tetrabutyl ammonium hexafluorophosphate (TBAP; Aldrich), and acetonitrile (Finar) were used without further purification. A three-electrode electrochemical cell setup with Cu foil (0.1-mm thickness) of 0.70 cm^2 as a working electrode, platinum as the counter electrode, and Ag wire as a pseudoreference electrode was used for electrodeposition of CuPc. Initially,

potentiodynamic experiments were conducted to determine the copper oxidation potential in acetonitrile containing only TBAP. An electrolytic bath containing Li_2Pc (0.01 M) and TBAP (0.1 M) in acetonitrile was used for electrochemical growth of CuPc on copper electrode. Potentiostatic electrodeposition was carried out from the above electrolytic bath at 0.075 V versus Ag wire, for 5 min. Thin film grown on the surface was washed with acetonitrile and used for further electrochemical, surface, structural, and spectroscopic investigations. The potentiostatic electrodeposition (−0.9 V vs Ag/AgCl) of Cu on indium tin oxide (ITO) electrode was done using $CuSO_4$ (0.1 M) containing Na_2SO_4 (0.5 M) as supporting electrolyte. As described earlier, a similar procedure was adapted to electrodeposit CuPc on ITO/Cu surface. In addition, a bare ITO electrode electrodeposited with LiPc thin film was used for comparative analysis.

The surface morphology of the electrodeposited sample was observed using FESEM-ZEISS Ultra-55. Thin-film X-ray diffraction pattern was recorded in Rigaku Smartlab diffractometer at the grazing angle and normal incidence. UV-visible spectra of ITO-LiPc and ITO/Cu-CuPc were measured using Thermo Scientific Evolution 201. The grazing angle Fourier transform infrared (FTIR) spectrum was measured using PerkinElmer FTIR Spectrum GX. All electrochemical preparations and characterizations were done using CH Instruments CHI-6008E. HER on copper and CuPc coated electrodes were done in 0.1 M HCl in a three-electrode cell setup. Potentiostatic impedance measurements were carried out at open circuit voltage and under hydrogen evolution condition at −0.7 V versus Ag/AgCl in the frequency range of 100 kHz to 0.1 Hz with 5-mV amplitude for copper and CuPc covered copper electrodes. Photoelectrochemical HER was performed with one side illumination on the surface of the photocathode using Xenon Arc lamp source (400 W). The photocurrent measurement of CuPc on the copper electrode was measured in open circuit voltage (−0.05 V vs Ag/AgCl) in 0.5 M Na_2SO_4 solution.

Results and discussion

The cyclic voltammograms (CVs; Fig. 1) are illustrative for the choice of potential (0.075 V) for concurrent electrooxidation of Li_2Pc and copper. Here, in the CV curve, (1) an electrooxidation peak (shown marked with asterisk) is observed with the electrolyte containing Li_2Pc. Following this peak, there is a continuous increase in anodic current density. This is attributed to the continuous release of copper ions from the Cu electrode. The electrooxidation of Li_2Pc on non-reactive electrodes (Pt, Au, ITO, and SS) show a clear electrooxidation peak, which is discussed in earlier reports [26–28]. The curve 2 in Fig. 1 illustrates the bare copper
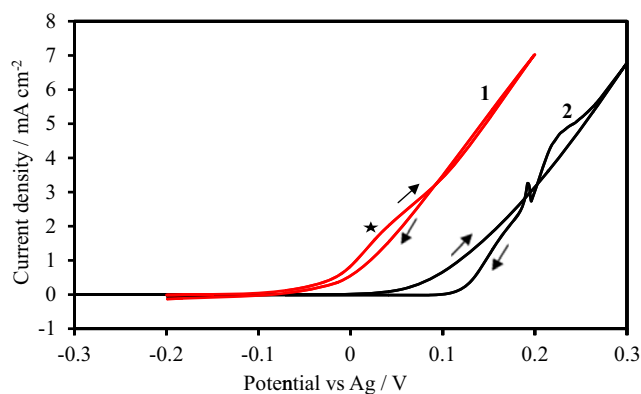
Fig. 1 Cyclic voltammograms of Cu electrode (*1*) in acetonitrile containing 0.01 M Li$_2$Pc and 0.1 M TBAP at a sweep rate of 10 mV s^{-1} and Cu electrode (*2*) in acetonitrile containing 0.1 M TBAP at the sweep rate of 10 mV s^{-1}. *Arrows* show the forward (*upward arrow*) and reverse (*downward arrow*) scan. A *star* shows the peak

oxidation in the electrolyte without Li$_2$Pc. Comparison of curves 1 and 2 suggests the close potential regime for electrooxidation of both Li$_2$Pc and Cu. Hence, in this approach, copper acts as a reactive working electrode. In addition, there is a small cathodic shift on the onset electrooxidation potential in the electrolyte containing Li$_2$Pc. From the CV analysis, the potential values were chosen to favor the simultaneous electrooxidation of both Li$_2$Pc and Cu. It is well known that M^{2+} ion can easily replace both the Li$^+$ ions of Li$_2$Pc in the solution. Here the electrooxidation of Li$_2$Pc yields LiPc radical which can readily react with copper ions (Cu^{1+}) which were released from the electrode surface. Moreover, LiPc radical is well known to undergo easy reduction [26–28]. Here the LiPc radical is reduced by oxidation of anodically generated Cu^{1+} to Cu^{2+} near the electrode/electrolyte interface. These Cu^{2+} ions

easily displace the lithium ions in phthalocyanine core near the interface, and concurrently, the growth of CuPc is observed on the electrode surface. Hence, there is a stringent necessity to have control of the electrooxidation potential of copper surface and Li$_2$Pc from the solution to favor the growth of CuPc. Since, as the electrooxidation potentials were increased by potentio-dynamic or potentiostatic methods, a swift precipitation was observed inside the electrolytic bath. This is due to the extensive release of copper ions into the solution and faster rate of formation of CuPc in the solution than on the electrode. CuPc formed in the solution appears turbid and settle down in the bottom of the electrochemical cell. Moreover, the electrolytic solution turns to pale or even colorless within few minutes. The analysis of the settled products shows the similar spectroscopic and structural characteristics of CuPc. Furthermore, at higher electrooxidation potentials (>0. 15 V in Fig. 1), no proper film formation was observed on the electrode surface. The choice of the anodization potential range (0.02 to 0.09 V) in the given electrolytic bath condition controls the co-electrooxidation of copper substrate and Li$_2$Pc followed by near electrode surface reaction favors the growth of CuPc thin film on the working electrode. Similar experiments were performed on ITO electrodeposited with the copper thin film (ITO-Cu) electrode yielding a bright cyan color ITO/Cu-CuPc. However, the electrooxidation of Li$_2$Pc on the bare ITO surface produces dark greenish LiPc thin films. Both the electrodes are visibly distinct in color and support the above growth process of CuPc on copper electrode.

The scanning electron micrograph (Fig. 2) of CuPc covered on copper exhibits nanorod-like features. These nanostructure growth further facilitates the continuous anodic release of copper ions from copper surface and subsequent growth of CuPc.

Fig. 2 Scanning electron micrograph of CuPc film on the copper surface showing nanorod-like structures. The *inset* shows a photograph of electrodeposited CuPc film on copper electrode
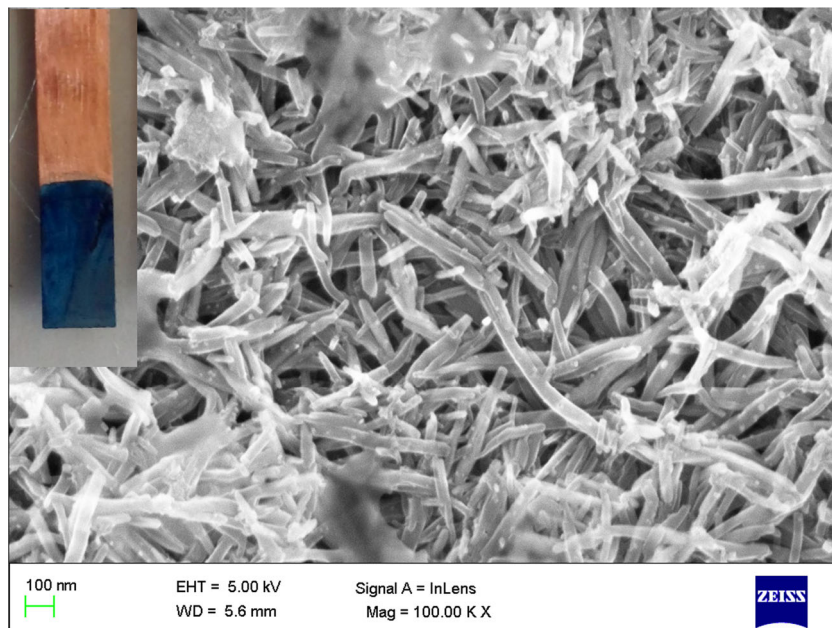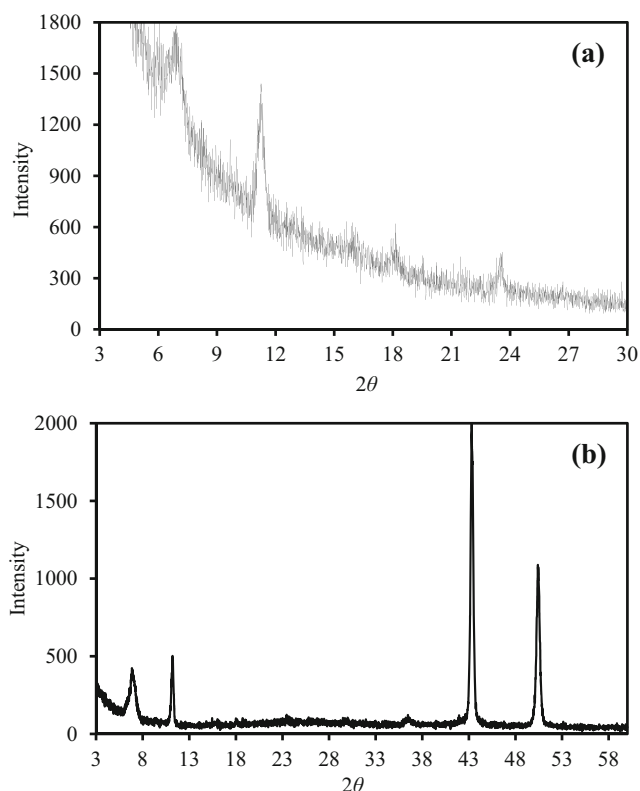
Fig. 3 Thin-film X-ray diffraction patterns of CuPc film on the copper surface. **a** Grazing angle incidence. **b** Normal angle incidence
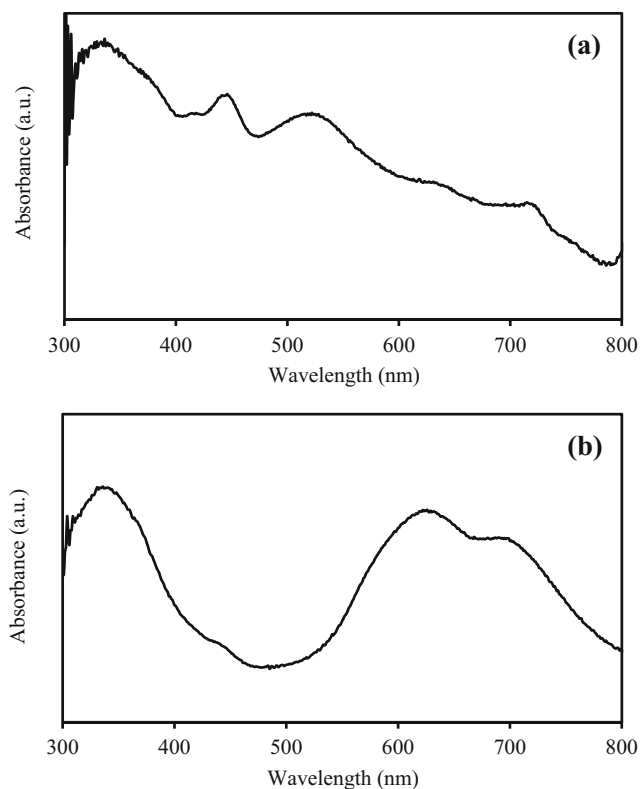

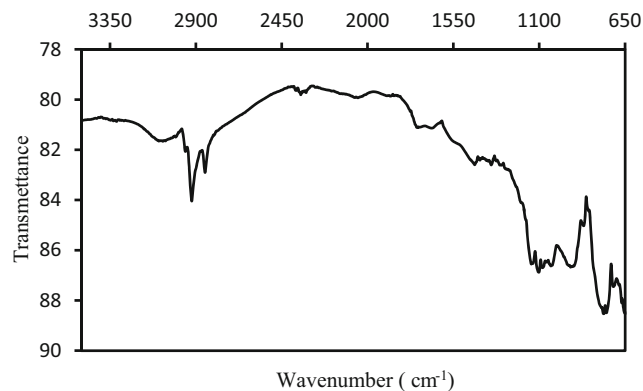**Fig. 4** UV-visible absorption spectra. **a** LiPc coated on ITO glass. **b** CuPc coated on ITO glass

Fig. 5 Grazing angle FTIR spectrum of electrochemically grown CuPc film on the copper surface

Inset of Fig. 2 is the photographic image of CuPc on the copper electrode showing bright cyan color which is similar to CuPc prepared by reacting Li_2Pc and Cu^{2+} in solution. The X-ray diffraction patterns (Fig. 3a, b) confirm the thin-film phase α-CuPc. The diffraction peak at 2θ value of 6.9 corresponds to the highest intense peak of metastable α phase. This is assigned to 002 lattice plane with the intermolecular distance of 3.79 Å in α-CuPc (4.79 Å in β-CuPc). Notably, the diffraction pattern does not show any additional intense peak at 9.19 (−102), which confirms the absence of β-CuPc. The other peaks also well correlate to α-CuPc, as reported in the literature [18, 19, 31]. Additional intense peaks at 43.5 and 50.5 correspond to the base copper substrate (PDF no 1–1241). In CuPc, α (metastable) to β (stable) transitions are known to appear at high temperatures (>250 °C) and due to solvent effects [31]. CuPc thin film fabricated by high-temperature methods normally exhibits β modification [31]. Here, the room temperature electrochemical synthesis yields nanocrystalline α-CuPc, which is not common in many fabrication techniques. The grazing angle incidence (Fig. 3a) shows the difference in the intensities of the peaks to that of normal incidence. This is due to the preferential orientation of
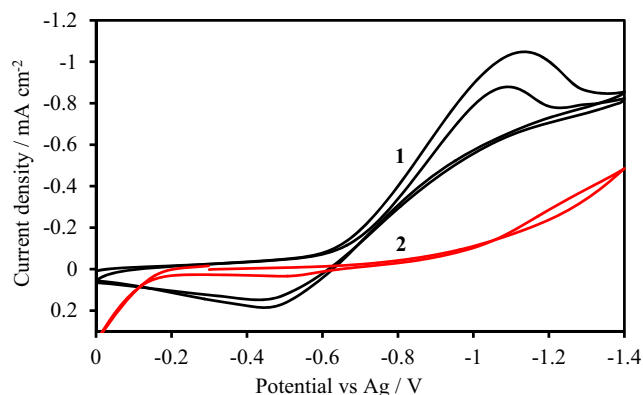

Fig. 6 Cyclic voltammograms of CuPc coated on Cu electrode (*1*) and bare copper (*2*) in acetonitrile containing 0.1 M TBAP at the sweep rate of 10 mV s^{-1}
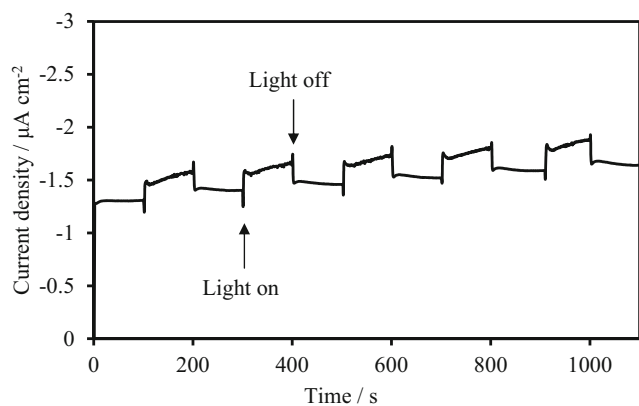
Fig. 7 The photocurrent measurement of CuPc electrodeposited on the Cu electrode measured at open circuit voltage (−0.05 V vs Ag/AgCl) in 0.5 M Na_2SO_4 solution

phthalocyanine crystallites. Figure 4a, b shows the UV-vis spectra of ITO coated with LiPc and Cu-CuPc, respectively. In Fig. 4b, the B (335 nm; d–π* transitions) and Q (615 and 700 nm; π–π* transitions) bands agree well with the reported CuPc spectrum [32]. The UV-vis spectrum (Fig. 4a) of electrodeposited LiPc on bare ITO shows that distinct band positions with additional bands at lower wavelength are in good
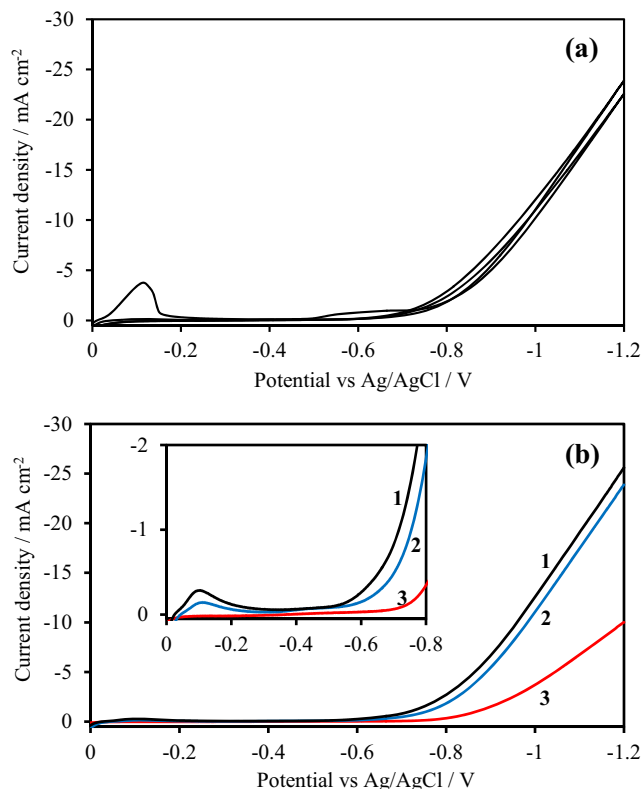
agreement with reported literature [27]. The grazing angle FTIR spectrum (Fig. 5) of CuPc on copper shows the characteristic vibrations corresponding to C–N (1102 cm^{-1}), C=N (1600 cm^{-1}), C=C (1650 cm^{-1}), =C–H (3000–3100 cm^{-1}), and C–H (2800–3000 cm^{-1}). There is no strong band observed at 3400–3200 cm^{-1} region which corresponds to the N–H antisymmetric stretching. This confirms that the thin film is metallated phthalocyanine and it is free from H_2Pc. Also, there is a blue shift in some of the bands due to metal incorporation into the phthalocyanine cavity [31].

Comparative CVs (Fig. 6) of CuPc coated on copper (1) and a bare copper (2) in the acetonitrile containing TBAP depict the redox behavior of phthalocyanine ring. Instead, the bare copper shows no similar characteristics. Copper electrode shows a small increase in current values at more negative potentials in the forward scan. This could be due to weak adsorption of tetrabutyl ions on the copper surface. In the reverse scan, an increase in current from −0.15 to 0 V was observed with the bare copper electrode. This signifies the easy electrooxidation of the uncoated copper surface. This behavior is absent in the CuPc covered copper surface which illustrates its electrochemical stability. Figure 7 shows a stable on–off photocurrent response of the nanostructured CuPc on
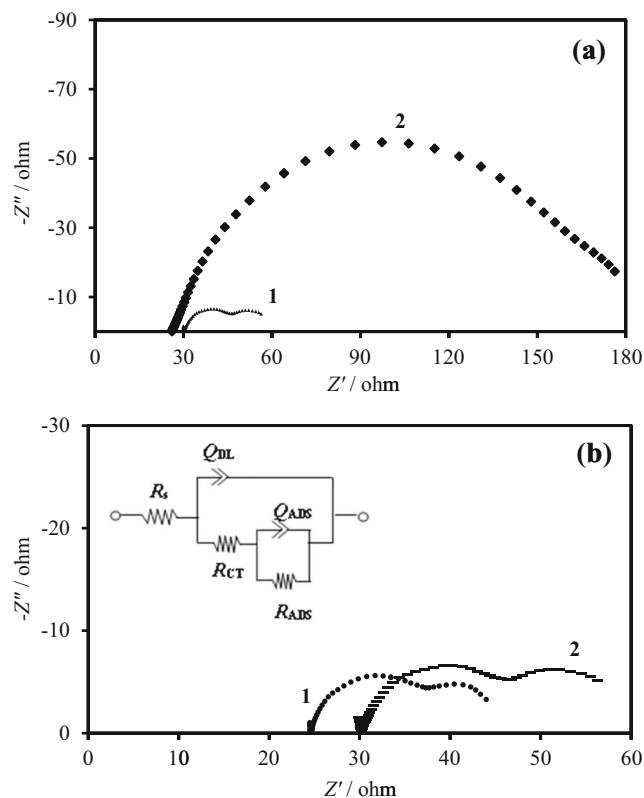

Fig. 8 **a** Cyclic voltammogram of CuPc coated on Cu electrode in 0.1 M HCl at a sweep rate of 10 mV s^{-1}. **b** A forward scan of the cyclic voltammograms of CuPc coated on Cu electrode under illuminated condition (*1*), CuPc on Cu electrode in dark (*2*), and bare Cu (*3*) in 0.1 M HCl at a sweep rate of 10 mV s^{-1}

Fig. 9 **a** Nyquist plots of CuPc deposited on Cu (*1*) and bare Cu (*2*) as working electrodes at −0.7 V vs Ag/AgCl (0.1 M KCl). **b** Nyquist plots of CuPc deposited on Cu electrodes under illuminated (*1*) and dark conditions (*2*) at −0.7 V versus Ag/AgCl (0.1 M KCl). The *inset* shows equivalent circuit for the hydrogen evolution reaction

copper in the neutral medium. Measurements carried out at open circuit potential show a significant cathodic photocurrent (0.25–0.35 $\mu A\ cm^{-2}$) generation. The photoresponses are reproducible over the long duration of measurements and even after the film reduction. The nanostructured CuPc thin films facilitate the ease separation of photogenerated charge carriers and it impedes the recombination process. The HER studies were done on the copper electrode and CuPc coated electrode (Fig. 8) showing higher stability in acidic conditions and an enhanced activity for hydrogen evolution on CuPc covered electrode. The first reduction peak at −0.12 V in the first cycle (Fig. 8a) of the CV does not reappear in the consecutive reduction cycles. This is due to the reduction of CuPc, and this reappears when the working electrode potential is reversed to positive electrooxidation potentials. In comparison to the bare copper electrode (Fig. 8b, curve 3), there is an increase in current density and a positive potential shift (150 mV) for HER on CuPc coated electrodes (curves 1 and 2). This is clearly shown in the forward scan of voltammograms in the inset of Fig. 8b. In photoelectrochemical HER, CuPc electrode exhibits a positive potential shift of almost 30 mV in comparison to dark condition (Fig. 8b). In addition, there is a considerable increase in the current density upon illumination of CuPc thin film. This infers the higher rate of charge transfer process across the interface. The potentiostatic impedance measurements are informative regarding the charge transfer resistance (R_{CT}) at photoelectrodes. The potentiostatic impedance spectrum (Fig. 9a) of the fresh copper electrode (2) shows more R_{CT} than CuPc on copper (1); this demonstrates that the photoelectrocatalytic hydrogen evolution of CuPc on copper is better than the uncoated copper surface. The inset of Fig. 9b shows the equivalent circuit for HER. The impedance spectra obtained with applied DC bias voltage (−0.7 V) is interpreted according to the proposed equivalent circuit for HER [32–34]. The impedance spectrum under illuminated (R_{CT} = 12 ohms) condition shows a better charge transfer for HER at −0.7 V than in dark condition (R_{CT} = 18 ohms) (Fig. 9b). Also, there is an increase in conductivity of the film under illumination which is observed at the high-frequency region. The high-frequency region Rs is attributed to the electrolyte and electrode resistive components. The R_{CT} corresponds to the charge transfer resistance for HER and C_{DL} to the capacitance in the first semicircle. The low-frequency semicircle corresponds to adsorption of reaction intermediates (H_{ADS}). Here the capacitive element is replaced with constant phase element (CPE—Q_{ADS}) due to surface roughness of the nanostructured electrode. R_{ADS} is pseudoresistance which is related to the mass transfer resistance of the adsorbed intermediate H_{ADS}, and Q_{ADS} is the pseudocapacitance. The overpotential assisted faster adsorption of H^+ on the copper phthalocyanine film, and faster desorption after charge transfer results in reduced adsorption resistance (R_{ADS}) and capacitance (Q_{ADS}). The

comparison of the shapes of the impedance spectra reveals that the process is charge transfer controlled on both copper and CuPc on copper electrodes. The nanostructured CuPc on copper electrode shows a significant reduction in R_{CT} and R_{ADS}.

Conclusions

In summary, we have demonstrated here for the first time the novel electrochemical approach for the preparation of the nanocrystalline metastable α-CuPc thin film. The control on the potential for co-electrooxidation is essential for the growth of thin film on the electrode surfaces. The difficulty associated with the processibility of solution phase unsubstituted CuPc is avoided by this method. In contrast to high-vacuum and high-temperature thin-film deposition methods, this is soft and economical. The photoelectrochemical HER performance on the CuPc covered copper surface is relatively higher than in dark and uncoated copper electrode. The transparent semiconducting surfaces electrodeposited with copper can be used for electrochemical deposition of CuPc thin film. This approach could be a possible direct route for the preparation of other MPc thin films, provided the electrooxidation potential of both metal and Li_2Pc matches. Moreover, this route could be used for forming heterojunctions of CuPc with other inorganic semiconductors.

References

1. Fujishima A, Honda K (1972) Electrochemical photolysis of water at a semiconductor electrode. Nature 238:37–38
2. Graetzel M (2003) Dye-sensitized solar cells. J Photochem Photobiol C 4:145–153
3. Walter MG, Warren EL, McKone JR, Boettcher SW, Mi Q, Santori EA, Lewis NS (2010) Solar water splitting cells. Chem Rev 110:6446–6473
4. Tong H, Ouyang S, Bi Y, Umezawa N, Oshikiri M (2012) Nano-photocatalytic materials: possibility and challenges. Adv Mater 24:229–251
5. Krol RVD, Graetzel M (2012) Photoelectrochemical hydrogen production. Springer Science+Business Media 102:3–11
6. Lewis NS (2005) Chemical control of charge transfer and recombination at semiconductor photoelectrode surfaces. Inorg Chem 44:6900–6911
7. Perez MD, Borek C, Forrest SR, Thompson ME (2009) Molecular and morphological influences on the open circuit voltages of organic photovoltaic devices. J Am Chem Soc 131:9281–9286
8. Tada A, Geng Y, Wei Q, Hashimoto K, Tajima K (2011) Tailoring organic heterojunction interfaces in bilayer polymer photovoltaic devices. Nat Mater 10:450–455

9. Hanack M, Subramanian LR (1997) Handbook of organic conductive molecules and polymers. Wiley 1:687

10. Leznoff CC, Lever ABP (1993) Phthalocyanines: properties and applications. VCH Publishers 3:436

11. Schumann S, Hatton RA, Jones TS (2011) Organic photovoltaic devices based on water-soluble copper phthalocyanine. J Phys Chem C 115:4916–4921

12. Chaure NB, Pal C, Barard S, Kreouzis T, Ray AK, Cammidge AN, Chambrier I, Cook MK, Murphy CE, Cain MG (2012) A liquid crystalline copper phthalocyanine derivative for high performance organic thin film transistors. J Mater Chem 22:19179–19189

13. Yu WL, Pei J, Cao Y, Huang W (2001) Hole-injection enhancement by copper phthalocyanine (CuPc) in blue polymer light-emitting diodes. J Appl Phys 89:2343–2350

14. Deon M, Caldas EM, Rosa DS, Menezes EW, Dias SLP, Pereira MB, Costa TMH, Arenas LT, Benvenutti EV (2014) Mesoporous silica xerogel modified with bridged ionic silsesquioxane used to immobilize copper tetrasulfonated phthalocyanine applied to electrochemical determination of dopamine. J Solid State Electrochem 19:2095–2105

15. Minami N (1982) Photocurrent spectra of phthalocyanine thin-film electrodes in the visible to near-infrared. J Chem Soc Faraday Trans 2(78):1871–1880

16. Couves JW, Tamizi M, Wright JD (1990) Photocurrent kinetics of group III metal–(phthalocyaninato)–halogen complexes in vacuum and oxidising gas atmospheres. J Chem Soc Faraday Trans 86:115–121

17. Richard JCB, Anthony RK (2005) The photoelectrochemistry of platinum phthalocyanine films in aqueous media. J Solid State Electrochem 9:459–468

18. Nonaka T, Nakagaw Y, Mori Y, Hirai M, Matsunobe T, Nakamura M, Takahagi T, Ishitani LH, Koumotob K (1995) Epitaxial growth of α-copper phthalocyanine crystal on Si(001) substrate by organic molecular beam deposition. Thin Solid Films 256:262–267

19. Wael KD, Westbroek P, Bultinck P, Depla D, Vandenabeele P, Adriaens A, Temmerman E (2005) Study of the deposition and Raman and XPS characterization of a metal ion tetrasulphonated phthalocyanine layer at gold surfaces: density functional theory calculations to model the vibrational spectra. Electrochem Commun 7:87–96

20. Koca A (2009) Copper phthalocyanine complex as electrocatalyst for hydrogen evolution reaction. Electrochem Commun 11:838–841

21. Standke B, Jansen M (1986) Ag3O4, the first silver (II, III) oxide. Angew Chem Int Ed Engl 25:77–78

22. Freyland W, Aravinda CL, Borissov D (2007) nanoscale electrocrystallization of metals and semiconductors from ionic liquids. In: Staikov G (ed) Electrocrystallization in nanotechnology. WILEY-VCH Verlag GmbH & Co. KGaA, Weinheim, pp 79–95

23. Milchev A (2002) Electrocrystallization: fundamentals of nucleation and growth. Springer Science & Business Media

24. Schlesinger TE, Rajeshwar K, Tacconi NRD (2010) Modern electroplating. Wiley, p 383–411

25. Xiao F, Hangarter C, Yoo B, Rheem Y, Lee K, Myung NV (2008) Recent progress in electrodeposition of thermoelectric thin films and nanostructures. Electrochim Acta 53:8103–8117

26. Sugimoto H, Mori M, Masuda H, Taga T (1986) Synthesis and molecular structure of a lithium complex of the phthalocyanine radical. J Chem Soc Chem Commun 962–963

27. Brinkmann M, André JJ (1999) Electrodeposited lithium phthalocyanine thin films. Part II:† magnetic properties and mesoscopic effects. J Mater Chem 9:1511–1520

28. Sakthivel K, Munichandraiah N, Scanlon LG (2005) Electrodeposition of adherent films of lithium phthalocyanine on platinum and stainless steel substrates by oxidation of dilithium phthalocyanine. J Electrochem Soc 152:C756–C763

29. Wang K, Dai L, Liu Q, Li H, Ju C, Wu J, Li H (2011) Electrodeposition of unsubstituted iron phthalocyanine nanostructure film in a functionalized ionic liquid and its electrocatalytic and electroanalysis applications. Analyst 136:4344–4349

30. Shrestha NK, Kohn H, Imamura M, Irie K, Ogihara H, Saji T (2010) Electrophoretic deposition of phthalocyanine in organic solutions containing trifluoroacetic acid. Langmuir 26:17024–17027

31. Defeyt C, Vandenabeele P, Gilbert B, Pevenage JV, Clootse R, Strivaya D (2012) Contribution to the identification of α-, β- and ε-copper phthalocyanine blue pigments in modern artists' paints by X-ray powder diffraction, attenuated total reflectance micro-fourier transform infrared spectroscopy and micro-Raman spectroscopy. J Raman Spectrosc 43:1772–1780

32. Armstrong RD, Henderson M (1972) Impedance plane display of a reaction with an adsorbed intermediate. J Electroanal Chem 39:81–90

33. Danaeea I, Noori S (2011) Kinetics of the hydrogen evolution reaction on NiMn graphite modified electrode. Int J Hydrog Energy 36:12102–12111

34. Lopes T, Andrade L, Ribeiro HA, Mendes A (2010) Characterization of photoelectrochemical cells for water splitting by electrochemical impedance spectroscopy. Int J Hydrog Energy 35:11601–11608